FULL TITLE
ASP Conference Series, Vol. **VOLUME**, **YEAR OF PUBLICATION**
NAMES OF EDITORS

Helioseismic Measurement of Large-Scale Solar Flows

M. F. Woodard

CoRA Division, NorthWest Research Associates, Inc.,
3380 Mitchell Lane, Boulder, CO 80301-5410 USA

Abstract. Large-scale flows in the deep convection zone, differential rotation and meridional circulation in particular, are relatively accessible to seismic probing and provide observational constraints on convection zone dynamics and structure. Flows and other aspherical perturbations dynamically couple the Sun's normal oscillation modes. Mode coupling produces signatures in power spectra of time series of coefficients in the spherical harmonic decomposition of the photospheric velocity field, the outstanding signature being the consequence of azimuthal-order (m) dependence of the mode frequencies, due to differential rotation. Mode coupling also produces a signature in cross spectra of distinct spherical harmonic time series. In this paper I discuss the problem of using helioseismic cross-spectra to map large-scale flow in the Sun and prospects for measuring deep meridional flow. Some preliminary estimates of meridional and zonal flow from MDI and GONG spherical harmonic time series are presented.

1. Introduction

Meridional circulation and zonal flow (differential rotation) are important players in the dynamics of the convection zone (CZ) and are currently under intense observational and theoretical scrutiny. The zonal flow is by far the most energetic flow pattern and strongly influences, via the Coriolis effect, many scales of convection. The zonal velocity pattern is in turn shaped by the turbulent transport of angular momentum in the CZ (12). Shear layers in the zonal velocity field are believed to be important in generating magnetic flux (7). Meridional flow can globally redistribute heat, angular momentum, and magnetic fields within the CZ on solar-cycle timescales. Meridional flow is of particular interest for flux transport dynamos (16). The model of Dikpati *et al.* (4), for instance, requires an equatorward flow of $3 - 5\,\mathrm{ms}^{-1}$ near the base of the CZ.

Information about the Sun's internal rotation comes mainly from measurements of the frequencies of oscillation modes of the entire Sun. Frequency analysis reveals layers of strong radial shear – the tachocline layer at the bottom of the CZ and a shear layer near the surface. One or both of these layers may be important in the magnetic dynamo. For the study of non-zonal flows global frequency analysis has not proven to be a useful tool, as distinct frequency signatures of these much weaker flows have yet to be identified. Information about subsurface meridional flow and smaller-scale flows comes mainly from local helioseismic analysis, an excellent overview of which can be found in (8). Local seismic methods include: ring analysis, which uses measurements of the local frequency-wavevector relation of waves, Fourier-Hankel spectral methods, which are closely related to partial-wave analysis, time-distance analysis, which

is related to (geo)seismic tomography, and helioseismic holography, an analog of optical holography.

Because of its importance for flux-transport dynamo models, the focus of this paper will be on meridional flow. A simple conveyor-belt picture of meridional flow has emerged from local seismic analysis, involving upwellings of gas near the equator compensated by downwellings near the poles. Poleward flows of order $15\,\mathrm{m\,s^{-1}}$ are seen in the outer CZ (9; 6; 1). The flow velocity in the deep convection zone is not as observationally well- constrained as the near-surface velocity and inferences from helioseismic analysis depend on assumptions about the nature of the flow near the bottom boundary. For instance, the most exhaustive study to date (5) shows equatorward flow in the tachocline if a mass-conserving constraint is obeyed, but without the constraint a poleward flow is obtained.

This paper describes an approach to inferring interior flows which uses cross spectra of distinct spherical harmonic amplitudes of the observable oscillation signal. Similar methods have been used in the analysis of supergranular- scale flow (19). A very preliminary analysis of GONG and MDI spherical harmonic time series is described along with tentative results for meridional flow.

2. Global Cross-Spectral Analysis

Cross-spectra of spherical harmonic time series are sensitive to flows and other aspherical solar structure. Global cross-spectral analysis is an extension of conventional power spectral analysis in that it uses 'covariance' data in the form $\varphi_{l'm'\omega'}\,\varphi^*_{lm\omega}$, where the amplitude $\varphi_{lm\omega}$ is the coefficient in the decomposition of the observed oscillation signal $\varphi(\hat{\mathbf{r}},t)$, as a function of heliographic coordinates and time, into spherical harmonic (l,m) and temporal frequency (ω) components. For the observational analysis described below, the observable signal is a spatially apodized photospheric Doppler velocity measurement.

With suitable frequency filtering, spherical harmonic amplitudes are proxies for normal-mode amplitudes, $a_\alpha\,(\alpha \equiv nlm)$, defined by the expansion

$$\mathbf{v}(\mathbf{r},t) = \sum_\alpha a_\alpha(t)\,\boldsymbol{\xi}_\alpha(\mathbf{r}) \tag{1}$$

of the internal oscillatory velocity field in mode velocity eigenfunctions of a spherically-symmetric non-rotating Sun. The sensitivity of cross-spectral data to internal flows is a consequence of the dynamical coupling of normal modes by the flows.

Because oscillation data do not sample the Sun uniformly, the observed spherical harmonic amplitudes do not completely isolate the contributions of individual modes but are related to the mode amplitudes by a leakage matrix. The lack of observations from the far hemisphere of the Sun is the main source of leakage and limits our ability to discriminate between modes for which l and m differ by small integers. The fact that the oscillatory signal originates in a thin layer of the solar atmosphere implies a similar overlap in n, however the n overlap problem is alleviated by the strong dependence of mode frequency on radial order. The leakage pattern is further complicated by the fact that only the line-of-sight component of velocity is observed and by temporal gaps in the data stream.

2.1. Forward Modeling

Forward modeling is an important step in the rigorous analysis of cross-spectral data. The cross-spectral forward modeling task consists of two independent subtasks: 1) computing the wave covariance matrix, $E[a_{\alpha'\omega'}\, a^*_{\alpha\omega}]$, for a solar model with specified flows, and 2) computing the leakage matrix, which relates the spherical harmonic and wave amplitudes, needed to convert wave covariance to spherical harmonic covariance $E[\varphi_{l'm'\omega'}\, \varphi^*_{lm\omega}]$.

The wave covariance model used in the present analysis is a global analog of a model (18) developed for helioseismic analysis of local, supergranular-scale flow. The model covariance $E[a_{\alpha'\omega'}\, a^*_{\alpha\omega}]$ is the sum of a zeroth-order contribution, $E[a_{\alpha'\omega'}\, a^*_{\alpha\omega}]_0$, appropriate for the reference model, and a perturbation $\delta E[a_{\alpha'\omega'}\, a^*_{\alpha\omega}]$, describing the mode-coupling contribution of flows. For sufficiently weak flows, the perturbation can be assumed to have a linear dependence on the flow velocity.

For the present analysis, I assume that the solar modes are excited independently. In this approximation the only non-zero wave covariances are the expected (limit) mode amplitude spectra $E[|a_{\alpha\omega}|^2]_0$. The zeroth-order limit spectra are represented by approximately Lorentzian frequency profiles defined by mode frequencies, widths, and power amplitudes characteristic of the reference model.

To linear order in the flow velocity, $\mathbf{u}(\mathbf{r}, t)$, the wave covariance perturbation takes the form

$$\delta E[a_{\alpha'\omega'}\, a^*_{\alpha\omega}] = -R_{\alpha'\omega'}\, \Lambda_{\alpha'\omega',\alpha\omega}\, E[|a_{\alpha\omega}|^2]_0 - R^*_{\alpha\omega}\, \Lambda^*_{\alpha\omega,\alpha'\omega'}\, E[|a_{\alpha'\omega'}|^2]_0, \qquad (2)$$

where the factor $R_{\alpha\omega}$ is the frequency response of the amplitude of mode α to a generalized harmonic driving force, while the coefficient $\Lambda_{\alpha'\omega',\alpha\omega} = -2i\omega \int dm\, \boldsymbol{\xi}^*_{\alpha'}(\mathbf{r}) \cdot \mathbf{u}_{\omega'-\omega} \cdot \nabla\, \boldsymbol{\xi}_\alpha(\mathbf{r})$ quantifies the strength with which global oscillation modes α and α' are coupled by the flow. The integral for $\Lambda_{\alpha'\omega',\alpha\omega}$ is taken over the entire Sun, with dm denoting an element of mass and $\mathbf{u}_\omega(\mathbf{r})$ the temporal Fourier transform of the flow velocity $\mathbf{u}(\mathbf{r}, t)$. I use the discrete Fourier convention $f(t) = \sum_\omega f_\omega \exp(-i\omega t)$ to represent quantities during the time span $0 < t < T$ of observations used in the analysis. The eigenfunction normalization $\int dm\, \boldsymbol{\xi}^*_\alpha(\mathbf{r}) \cdot \boldsymbol{\xi}_\alpha(\mathbf{r}) = 1$ is assumed. The eigenfunctions used for the present analysis were computed from model S of Christensen-Dalsgaard *et al* (3).

The task of inverting data for subsurface flow is greatly simplified when the data depend linearly on the flow velocity. That the perturbation $\delta E[a_{\alpha'\omega'}\, a^*_{\alpha\omega}]$ due to solar large-scale flows can be adequately approximated by linear theory is questionable, mainly because the m-dependent splitting of the mode frequencies by differential rotation has a rather striking signature in the observed global oscillation spectrum, particularly at high degree. The above expressions for wave covariance were derived from a wave equation containing terms which describe the pairwise dynamical coupling of modes by a flow. From a mathematical standpoint, the frequency splittings are a consequence of terms which describe the coupling of modes to themselves. Therefore a straightforward, though somewhat artificial, way to improve the linearity of the forward model, would be to treat the flow-dependent self-coupling terms as part of the zeroth-order term rather than as a perturbation. This redefinition of the perturbation does not affect the above expressions for wave covariance. However, it does imply that

rotationally split mode frequencies rather than the frequencies of a non-rotating model, are to be used in the expressions for the response functions $R_{\alpha\omega}$ and the zeroth-order wave spectra $E[|a_{\alpha\omega}|^2]_0$. Since the flow-dependent self-coupling terms are no longer part of the perturbation, it follows that $\delta E[|a_{\alpha\omega}|^2] = 0$. The mode cross-coupling strength due to solar differential rotation also increases with l, implying that the linearized cross-spectral model is limited to modes of sufficiently low degree. Estimates of the coupling strength suggest that the theory is adequate for modes of degree less than 100 considered in this analysis. In a more exact treatment, one would linearize about a differentially-rotating model, using mode eigenfunctions appropriate to that model (17; 14).

The forward model is strictly valid only in a Sun-centered inertial reference frame. However, because the GONG and SOHO instruments move in approximately circular trajectories with respect to an inertial frame, it is convenient to interpret quantities in the forward model (mode frequencies, flow velocities, etc.) in terms of a uniformly-rotating frame. In a more rigorous treatment, one would include Coriolis and centrifugal effects.

For the present analysis, the calculation of mode amplitude leakage is based on the following simplifying assumptions: 1) the oscillations are observed in a thin layer of the solar photosphere located approximately 200 km above the $\tau_{5000} = 1$ level, 2) GONG and MDI observe the line-of-sight component of the wave velocity $\mathbf{v}$, given by eq. (1) from corotating vantage points in the solar equatorial plane and I use coordinate systems in which the longitude of the observation points are zero, 3) the observed Doppler images have been apodized by a spatial cosine bell window, as described by Vorontsov and Jefferies (15), and 4) there are no temporal gaps in the data. Given a leakage matrix, the forward model of wave covariance can be straightforwardly turned into a model of spherical harmonic covariance, $E[\varphi_{l'm'\omega'}\,\varphi^*_{lm\omega}]$, equal to the sum of zeroth-order and perturbation contributions, $E[\varphi_{l'm'\omega'}\,\varphi^*_{lm\omega}]_0$ and $\delta E[\varphi_{l'm'\omega'}\,\varphi^*_{lm\omega}]$.

2.2. Comparing Observed and Theoretical Flow Signatures

The cross-spectral signatures of steady, axisymmetric meridional and zonal flows are of great interest in connection with dynamo models. Such flows couple mode amplitudes of the same m and ω and therefore it is instructive to consider cross spectra of the form $\varphi_{l'm\omega}\,\varphi^*_{lm\omega}$. The cross spectrum at fixed l and l' is conveniently displayed in the '$m-\nu$' format originally used to display the spectral signature of solar rotation (2).

As a consequence of leakage, the signature of flow is only a small contribution to the observed cross spectrum. An obvious way to extract the flow signature would be to subtract the theoretical zeroth-order expectation $E[\varphi_{l'm\omega}\,\varphi^*_{lm\omega}]_0$ from the observed cross spectrum. The resulting residual $m-\nu$ cross spectrum $\delta(\varphi_{l'm\omega}\,\varphi^*_{lm\omega})$ should resemble the flow-dependent perturbation $\delta E[\varphi_{l'm'\omega'}\,\varphi^*_{lm\omega}]$ computed for realistic solar flows. The analysis described in §2.3. is based on residual data. For the purpose of simply displaying flow signatures, however, I exploit a symmetry property of the leakage contribution which is robust at high-l. To remove the leakage signature I first shift the cross spectrum at each m to compensate the effect of the frequency shift due to differential rotation. Then I conjugate the $m-\nu$ cross spectrum, interchange $\varphi^*_{l'm\omega}\,\varphi_{lm\omega}$ and $\varphi^*_{l',-m,\omega}\,\varphi_{l,-m,\omega}$, and subtract the result from the original cross spectrum.

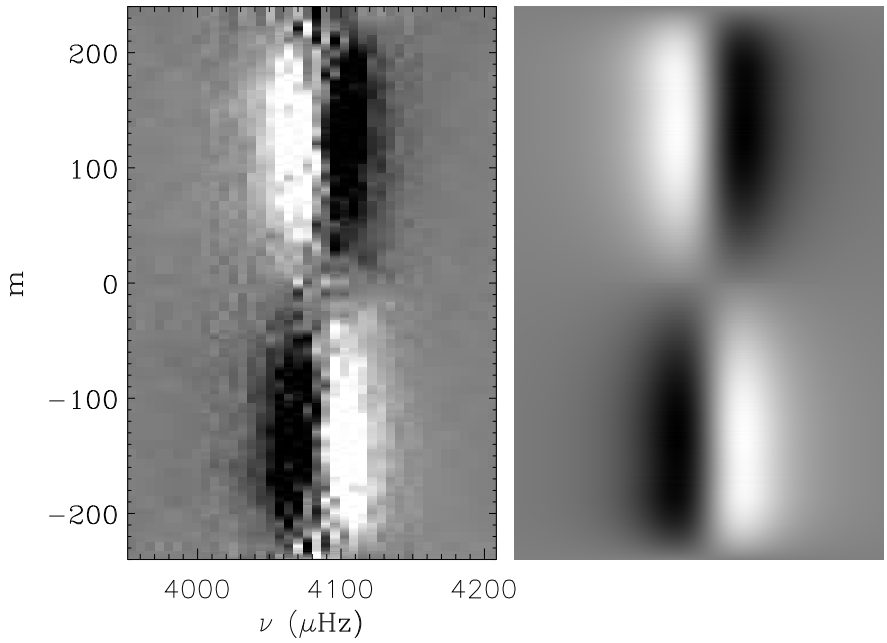

Figure 1. The real part of the observed and theoretical $m - \nu$ spectrum discussed in the text.

Cross spectra at large l for which l and l' differ by small integers are optimal for detecting meridional flow and the latitudinal variation of zonal flow. Examples of symmetrized observed and theoretical $m - \nu$ cross spectra, for $l = 240$ and $l' = 242$, are shown in Figures 1 and 2. The displayed cross spectra are dominated by mode-couplings for which $n' = n = 6$ and $l' = l \pm 2 \approx 240$ (the imprecision in l being a consequence of leakage). The observed cross spectra were derived from a 72-day sequence of spherical harmonic fit coefficients computed from MDI medium-l Doppler images beginning on 1996 July 12. The theoretical spectra were computed for a combination of meridional and zonal flows which are representative of the flows obtained from prior observational analysis. The fact that the signature of zonal flow is mainly real valued, while that of meridional flow is mainly imaginary, simplifies the analysis of observational data. Note that the noisy observed cross spectra have been smoothed to make the flow signatures more evident. Smoothing is particularly important in bringing out the weak signature of meridional flow: the imaginary part of the displayed spectrum is the result of smoothing over the entire range $-l < m < l$ of azimuthal order.

2.3. Preliminary Analysis of Meridional Flow

Rough estimates of the depth dependence of axisymmetric meridional flow were made from a 72-day sequence of simultaneous GONG and MDI spherical harmonic coefficients beginning on 1996 Sep 22. To represent flows I use the expansion in vector spherical harmonic functions of Lavely and Ritzwoller (11). In this expansion, the vector harmonics for meridional flow, and other poloidal flows,

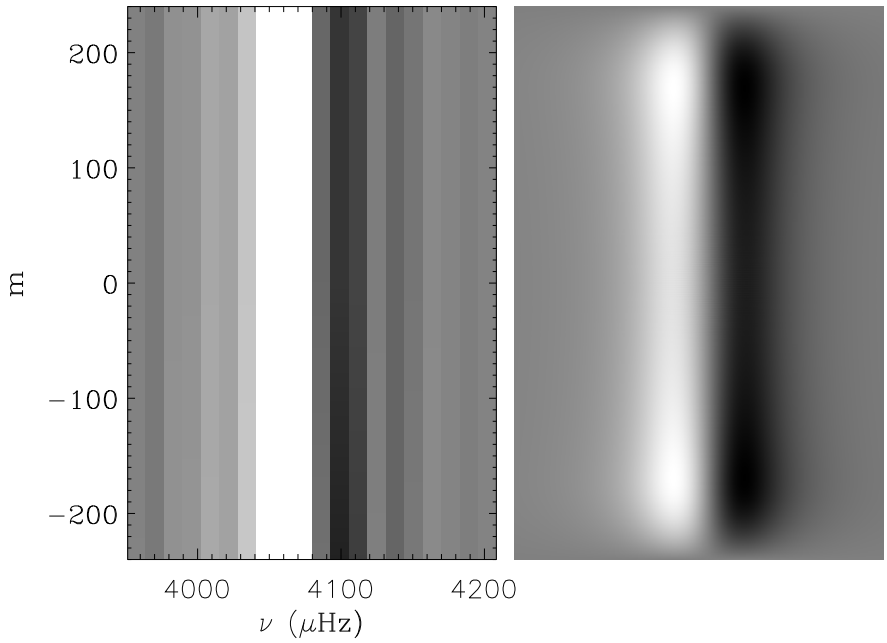

Figure 2. The imaginary part of the observed and theoretical $m - \nu$ spectrum discussed in the text.

take the form $u_s^t(r)\, Y_s^t(\theta,\phi)\, \hat{\mathbf{r}} + v_s^t(r)\, \nabla_1\, Y_s^t(\theta,\phi)$, where $\nabla_1 \equiv \hat{\boldsymbol{\theta}}\, \partial_\theta + \hat{\boldsymbol{\phi}}\, \partial_\phi / \sin\theta$ and Y_s^t denotes the scalar spherical harmonic function of degree s and order t. The functions u_s^t and v_s^t give the linear velocity amplitude of the radial and horizontal multipole components at each r. The dominant component of the observed meridional flow is a quadrupolar, $s = 2$, $t = 0$ pattern. The vector harmonics for zonal flow, and other toroidal flows, take the form $-w_s^t(r)\, \hat{\mathbf{r}} \times \nabla_1\, Y_s^t(\theta,\phi)$. Note that the w_1^0, w_3^0, w_5^0, .. functions, describing the latitude- independent component of rotation and various shear components, affect, respectively, the a_1, a_3, a_5, .. coefficients in terms of which oscillation frequency splittings are conventionally parameterized (13).

Cross spectral data were analyzed under the assumption that solar meridional flow is a simple quadrupolar pattern. The horizontal angular velocity of the pattern has the form $\gamma(r)\sin(2\theta)$. I ignore the radial component of the flow velocity, even though doing so violates the constraint of mass conservation. To characterize the depth dependence of the flow, I fit residual $m - \nu$ cross spectral data $\delta\,(\varphi_{l+2,m\omega}\, \varphi^*_{lm\omega})$ which target specific n and l values (e.g., Figure 1) to theoretical cross spectra $\delta E[\varphi_{l+2,m\omega}\, \varphi^*_{lm\omega}]$ computed for a quadrupolar flow pattern with a depth-independent angular velocity amplitude $\gamma(r) = \gamma_{nl}$. The γ_{nl} obtained from the fit targeting a particular (n,l) multiplet can be shown to be approximately a weighted average over r of $\gamma(r)$, where the weighting function is the fractional kinetic energy per unit r in modes of the targeted multiplet. Radially-averaged angular velocity amplitudes γ_{nl} were estimated for p-mode multiplets of l between 25 and 85 and frequencies in the approximate range $2 - 4$ mHz. Figure 3 shows the measured γ_{nl}, in nHz, as a function of

the relative inner turning radius of the modes of the multiplet, for GONG and MDI. The measurements have been smoothed in radius, to improve the signal-to-noise. Note that at $r = R_\odot$ an angular velocity of 1 nHz corresponds to a linear velocity of $\approx 4.4\ \mathrm{m\,s^{-1}}$.

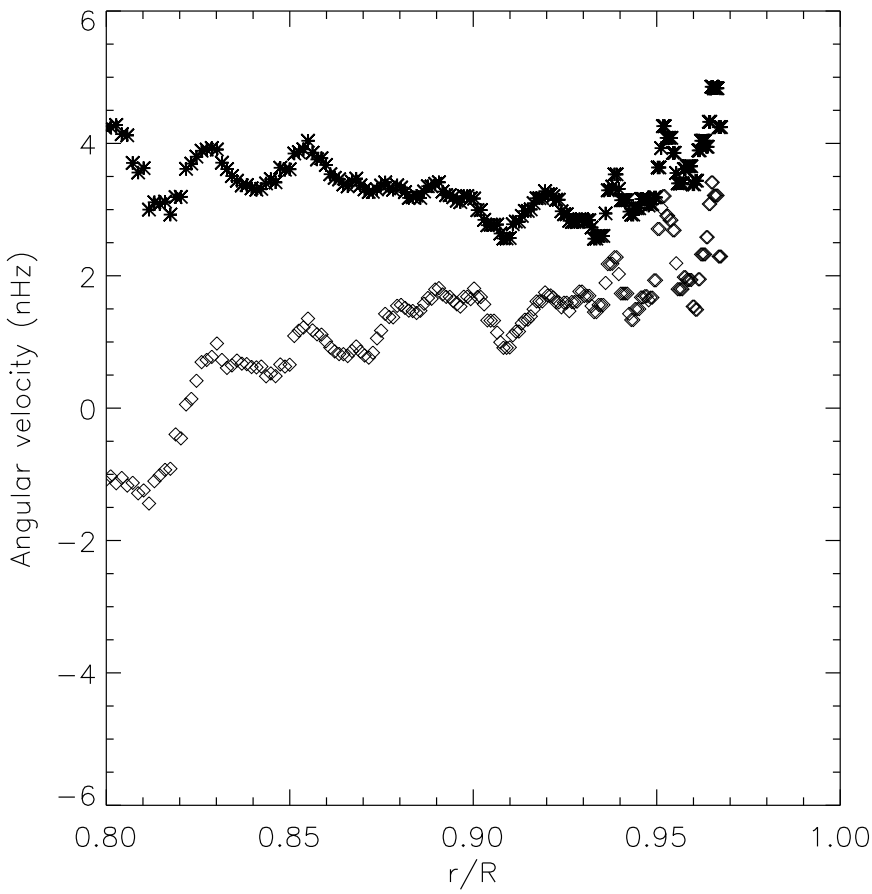

Figure 3. GONG (asterisks) and MDI (diamonds) meridional flow velocity measurements γ_{nl} as a function of relative turning radius.

While the GONG and MDI meridional flow rates are roughly consistent with one other and with previous measurements in the upper CZ, they clearly diverge for modes with turning radius deep in the CZ. (The detailed correspondence between the GONG and MDI curves is most likely the result of smoothed correlated noise fluctuations.) The source of the discrepancy is not known. There are certainly known systematic errors for which the flow estimates have not been corrected. An important source of error for waves with turning points deep in the CZ arises because of the variation across the solar disk in the time required for light originating in the solar atmosphere to reach helioseismic instruments. Another, potentially important, though not well studied, velocity artifact is expected to be present because of the combination of the disk varia-

tion in the height in the solar atmosphere at which oscillations are observed and non-adiabatic wave behavior at the observed height. The known effects should be the same for GONG and MDI, however. In these proceedings Duvall and Hanasoge present evidence of velocity artifacts in MDI data comparable in magnitude to light-delay effects, though of opposite sign. It is not clear whether such effects are present in GONG data or how they are related to the discrepancies shown in Figure 3.

3. Detectability of Meridional Flow

Cross-spectral analysis provides measurements of mode coupling, so it is illuminating to consider how the coupling strengths $\lambda_{\alpha'\alpha} \equiv \Lambda_{\alpha'\omega,\alpha\omega}/2\omega$ (see discussion of eq. [2]) for steady, axisymmetric flow depend on the flow velocity. As discussed earlier, the coupling of modes $\alpha = n\ell m$ and $\alpha' = n\ell' m$ with $\ell' = \ell + 2$ is of prime interest. For these modes the imaginary part of $\lambda_{\alpha'\alpha}$ is sensitive to quadrupolar meridional flow. The sensitivity to the v_2^0 profile, for $n, \ell, m = 5, 80, 40$, is shown in Figure 4. On the other hand, the real part of the coupling strength depends on the zonal flow velocity. The sensitivity of $Re\{\lambda_{\alpha'\alpha}\}$ to the w_3^0 function is almost identical (up to an overall scale factor of order unity) to the kernel shown for meridional flow.

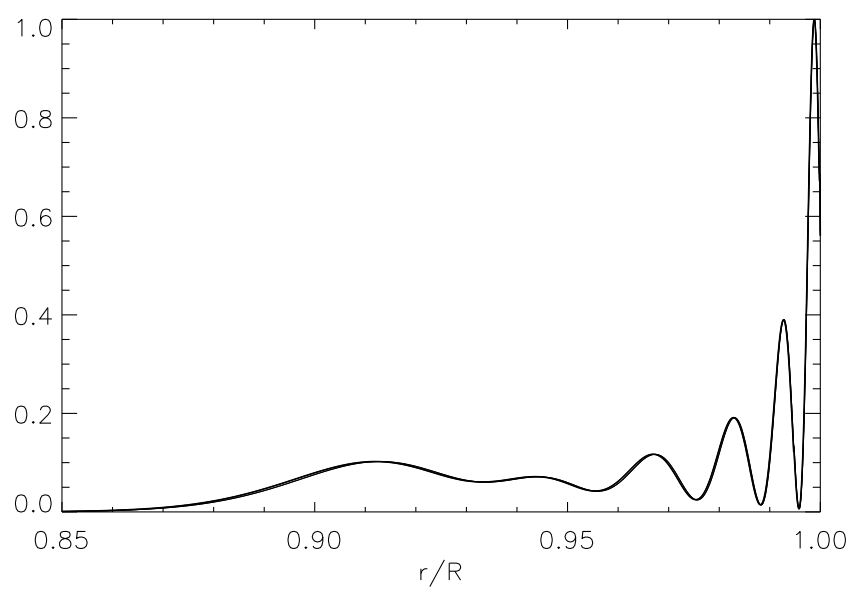

Figure 4. Rescaled coupling-constant sensitivity kernels

The mode coupling sensitivity kernels also strongly resemble the more familiar rotational splitting kernels. To linear order in the flow velocity, the frequency of an oscillation mode α is the (real-valued) self-coupling strength $\lambda_{\alpha\alpha}$. The sensitivity of mode frequency to the components w_1^0 and w_3^0 of differential rotation,

also shown in Figure 4 for $\alpha = 5, 80, 40$, is virtually ndistinguishable from the other coupling kernels.

The similarity of the kernels shown suggests that large-scale meridional flow can be detected at about the same level of statistical uncertainty and with similar depth resolution as the zonal flow. This suggestion is corroborated by (unpublished) analysis of the noise in cross-spectral measurements. Using published inversions of oscillation frequency splittings for zonal flow (10), I estimate that with 11 years of oscillation data the meridional flow speed near the base of the CZ can be determined with a $3\,\sigma$ uncertainty of approximately $2\,ms^{-1}$ and a vertical resolution of approximately 25 % of the depth of the CZ. Similar results have been obtained by Braun and Birch (these proceedings). The findings of this paper suggest that our knowledge meridional flow can be substantially improved, provided that the challenge of understanding systematic error can be met.

Acknowledgments. I thank Doug Braun, Yuhong Fan, Aaron Birch and others for stimulating discussions during the past decade and the SOC for the invitation to speak. The solar eigenfunctions used in this analysis were computed for Model S of Christensen-Dalsgaard *et al.* by Aaron Birch using the Aarhus Adiabatic Pulsation Package. A number of people, Jesper Schou and David Salabert, in particular, have provided technical support and advice. This project was supported by NASA under contract NAS5-03114. The Solar Oscillations Investigation-Michelson Doppler Imager experiment on *SOHO* is supported by NASA contract NAG 05-3077 and Stanford University. *SOHO* is a project of international cooperation between ESA and NASA. The GONG project is managed by the National Solar Observatory, a Division of the National Optical Astronomy Observatories, which is operated by AURA, Inc., under a cooperative agreement with the National Science Foundation.

References

1. D. C. Braun and Y. Fan. Helioseismic Measurements of the Subsurface Meridional Flow. ApJ, 508:L105–L108, November 1998.

2. T. M. Brown. Solar rotation as a function of depth and latitude. Nat, 317:591–594, October 1985.

3. J. Christensen-Dalsgaard, C. R. Proffitt, and M. J. Thompson. Effects of diffusion on solar models and their oscillation frequencies. ApJ, 403:L75–L78, February 1993.

4. M. Dikpati, G. de Toma, P. A. Gilman, C. N. Arge, and O. R. White. Diagnostics of Polar Field Reversal in Solar Cycle 23 Using a Flux Transport Dynamo Model. ApJ, 601:1136–1151, February 2004.

5. P. M. Giles. *Time-distance measurements of large-scale flows in the solar convection zone.* PhD thesis, Stanford University), August 2000.

6. P. M. Giles, T. L. Duvall, Jr., P. H. Scherrer, and R. S. Bogart. A Flow of Material from the Suns Equator to its Poles. Nat, 390:52, November 1997.

7. P. A. Gilman. Fluid Dynamics and MHD of the Solar Convection Zone and Tachocline: Current Understanding and Unsolved Problems - (Invited Review). Solar Phys., 192:27–48, March 2000.

8. L. Gizon and A. C. Birch. Local Helioseismology. *Living Reviews in Solar Physics*, 2:6, November 2005.

9. D. H. Hathaway. Doppler Measurements of the Sun's Meridional Flow. ApJ, 460:1027, April 1996.

10. R. Howe, J. Christensen-Dalsgaard, F. Hill, R. W. Komm, R. M. Larsen, J. Schou, M. J. Thompson, and J. Toomre. Dynamic Variations at the Base of the Solar Convection Zone. *Science*, 287:2456–2460, March 2000.

11. E. M. Lavely and M. H. Ritzwoller. The effect of global-scale gravitational asphericities on helioseismic oscillations. *Royal Society of London Philosophical Transactions Series A*, 339:431–496, 1992.

12. M. S. Miesch. The coupling of solar convection and rotation - (Invited Review). Solar Phys., 192:59–89, March 2000.

13. J. Schou, J. Christensen-Dalsgaard, and M. J. Thompson. On comparing helioseismic two-dimensional inversion methods. ApJ, 433:389–416, September 1994.

14. S. V. Vorontsov. Solar p modes of high degree l: coupling by differential rotation. MNRAS, 378:1499–1506, July 2007.

15. S. V. Vorontsov and S. M. Jefferies. Modeling Solar Oscillation Power Spectra. I. Adaptive Response Function for Doppler Velocity Measurements. ApJ, 623:1202–1214, April 2005.

16. Y.-M. Wang, N. R. Sheeley, Jr., and A. G. Nash. A new solar cycle model including meridional circulation. ApJ, 383:431–442, December 1991.

17. M. F. Woodard. Distortion of high-degree solar p-mode eigenfunctions by latitudinal differential rotation. ApJ, 347:1176–1182, December 1989.

18. M. F. Woodard. The Seismic Correlation Signature of Moderate-Scale Flow in the Su n. ApJ, 649:1140–1154, October 2006.

19. M. F. Woodard. Probing Supergranular Flow in the Solar Interior. ApJ, 668:1189–1195, October 2007.